



Cite this: *Chem. Commun.*, 2026, 62, 2097

Received 30th September 2025,
Accepted 8th December 2025

DOI: 10.1039/d5cc05628d

rsc.li/chemcomm

Emergent properties of supramolecular peptide assemblies

Álvaro Vila,  † Sela González  † and Ignacio Insua  *

The self-assembly of supramolecular monomers can change their chemical properties and produce emergent functions that are absent in their dispersed state. In this review article, we describe structural and functional material properties emerging from the self-assembly of peptides, which are based on interactions between neighbouring monomers and the supramolecular environments they create. The non-covalent cooperativity of peptides is here discussed in terms of emergent properties like catalysis, chiral amplification, hierarchical self-assembly and life-like function. These collective effects are rationalised by the monomer packing structure and reactive group proximity, providing a perspective of self-assembling peptide designs and supramolecular material applications, including our own contribution to this topic.

1. Introduction

Molecules with complementary geometry and affinity can aggregate in an orderly manner into a wide range of supramolecular structures. This process of self-assembly generates molecular arrays, where neighbouring monomers can influence one another in terms of physical and chemical properties.¹ In this regard, emergent properties are here defined as the

collection of structural and functional effects derived from clustering molecules together, which are absent in their dispersed monomeric state.² These phenomena include fundamental changes in chemical reactivity, like the stabilisation of monomers against hydrolysis in the assembled state^{3,4} or monomer-to-assembly pK_a shifts,^{5,6} and new collective functions, like catalysis,⁷ luminescence⁸ or motion.⁹ Such emergent properties arise from the supramolecular environments generated by self-assembly, where the conformation of monomers becomes restricted, and their solvation shell is greatly replaced by interactions between bound monomers. For example, the positioning of acidic or basic groups in hydrophobic domains disfavours their ionisation, resulting in a change of pK_a .^{10,11} The close packing of monomers in the assembled state allows

Centro Singular de Investigación en Química Biolóxica e Materiais Moleculares (CiQUS), Departamento de Farmacoloxía, Farmacia e Tecnoloxía Farmacéutica, Universidade de Santiago de Compostela, 15705, Santiago de Compostela, Spain.
E-mail: ignacio.insua.lopez@usc.es

† These authors contributed equally.



Álvaro Vila

Álvaro Vila graduated in chemistry with a master's in chemistry at the interface of biology and materials science from the University of Santiago de Compostela in Spain. Since early 2025 he has been a PhD student in the group of Ignacio Insua, under the co-supervision of Javier Montenegro. His PhD thesis explores the capabilities of peptide amphiphiles to emulate the behaviour of biological structures. His broader research interests

include supramolecular chemistry, peptide-based biomaterials and synthetic biology-inspired systems.



Sela González

Sela González graduated in pharmacy at the University of Santiago de Compostela, Spain, in 2024. She has been pursuing her PhD under the supervision of Ignacio Insua at the Centre for Research in Biological Chemistry and Molecular Materials (CiQUS), in the University of Santiago de Compostela, since October 2024. Her PhD focuses on responsive self-assembling peptides to produce supramolecular nanomaterials for biomedical application.





Fig. 4 Autocatalytic synthesis of the self-assembling peptide amphiphile dodecyl-F₂E-OH. The kinetic profile shows normalised product concentration over time with the characteristic sigmoidal shape of autocatalytic processes. Adapted with permission from ref. 74, copyright 2025, Wiley-VCH.

water-heptane medium, allowing the competitive selection of products from pools of amino acid precursors.⁷⁵

3. Structural amplification

Structural amplification refers to the transmission of monomer geometry to co-assembled neighbours and to the overall supramolecular ensemble, for example, leading to the formation of chiral⁷⁶ and porous⁷⁷ materials. Additionally, the segregation of polar and hydrophobic domains during assembly can amplify the amphiphilic character of a monomer, triggering new assembly modes hierarchically.⁷⁸ In this section, we will discuss several supramolecular effects stemming from the structural amplification of monomer geometry and physicochemical properties. While these concepts have been previously reviewed in isolation, we here provide a holistic view of their supramolecular origin, emphasising monomer packing order in amplifying molecular topology (*e.g.* stereochemistry, binding/non-binding domains and amphiphilicity) in the supramolecular assemblies produced.

3.1. Chiral amplification

The chirality of supramolecular assemblies is generally dictated by the stereochemistry of their constituent monomers, which can amplify their geometry to produce torsions in the resulting nanostructures. With all proteinogenic amino acids being chiral, except glycine, the inversion of the D/L configuration of a single residue can dramatically affect self-assembly and structural chirality by introducing conformational mismatches that destabilise secondary structure and steric zipping.⁷⁹ Similarly, changes in D/L amino acid composition can produce changes in the handedness and helical pitch of peptide nanosheets.⁸⁰ While some reports establish a 'C-term rule',⁸¹

meaning that the overall chirality of an assembly is primarily determined by the D/L configuration of the amino acids at the C-terminus, other works have found that the central core residues of the assembly control supramolecular chirality.⁸² D/L inversions can also modulate the chirality of catalytic nanofibres, resulting in higher yields and enantioselectivity in aldol reactions,⁸³ as also observed in other peptide assemblies with helical pitch-dependent catalysis.⁸⁴

Changes in amino acid sequence order can perturb chiral amplification by side chain packing mismatch (*i.e.* unfavoured steric, polar or electrostatic interactions). For example, in tetrapeptides containing phenylalanine (Phe) and alanine (Ala), Phe-Ala₂-Phe produced larger and wider fibre bundles than the analogue Ala-Phe₂-Ala, where bulkier Phe residues in the centre of the monomer may hinder fibre elongation (Fig. 5A).⁸² Changes in helical fibre handedness have been observed in peptides maintaining chirality at their alpha carbons, for example between Phe₃-Lys and Ile₃-Lys (Fig. 5B).⁸⁵ The distinct side chain geometry and bulkiness of Phe and Ile, with the latter having a second chiral centre at the beta carbon, thus result in opposite M/P helicity from these two peptides. Additionally, the incorporation of non-peptide units at different monomer positions can induce M/P inversions of helical assemblies, for example, using diethylene glycol⁸⁶ or trifluoromethyl⁸⁷ groups.

In co-assembled systems using more than one monomer, chiral amplification can follow the sergeants-and-soldiers principle, where chiral monomers impose spatial organisation over achiral ones, and the majority-rules principle, where the overall chirality of the assembly will be determined by the excess of one of the chiral monomers present.⁸⁸ For example, benzene-1,3,5-tricarboxamide monomers substituted with different amino acids can impose the chirality of their alpha carbon by the sergeant-and-soldiers effect over achiral monomers.⁸⁹ Despite being very interesting and potentially valuable for biomaterial applications, these strategies of chiral amplification remain heavily unexplored in peptides, probably due to the challenge



Fig. 5 Amplification of monomer chirality into supramolecular helicity. (A) Effect of amino acid order on chiral fibre assembly. Scale bars = 1 μ m. Adapted with permission from ref. 82, copyright 2021, Wiley-VCH. (B) Impact of amino acid substitution [*i.e.* isoleucine (I)] for phenylalanine (F)] on chiral fibre handedness and helical pitch. Reprinted with permission from ref. 85, copyright 2024, Springer Nature.



of engineering chiral control in monomers with so many stereocentres.

3.2. Packing gaps

The packing pattern of peptides can leave gaps in the resulting assemblies, generating porous supramolecular materials by amplification of non-binding monomer domains. While this is an intuitive concept, rational porous material engineering requires fine monomer design considerations, relying on rigid building blocks with binding and non-binding domains in specific orientations. In this regard, porous peptide assemblies have been obtained from helical monomers^{90,91} and β -sheet forming amyloids,⁹² where the secondary structure restricts monomer flexibility and helps present different topologies for self-assembly, while leaving non-binding surfaces exposed to the solvent to form the pores (Fig. 6). The size and physicochemical properties of these cavities can be tuned by changes in monomer structure, like sequence extensions or mutations at specific positions, which can be rationally designed to control polarity and potential interactions with guest molecules.⁷⁷ For example, tripeptides with alternating L-D-L chirality segregate all side chains on one face of the peptide backbone to create a hydrophobic binding surface, while leaving the other side of the backbone as an 'empty' non-binding domain to create pores (Fig. 1C).⁹³ Additionally, fluorination at phenyl positions of a similar heterochiral dipeptide, ^DPhe-^LPhe, affects binding interfaces by incorporation of halogen bonds, thereby modulating packing order and the viscoelastic properties of the material.⁹⁴

3.3. Hierarchical self-assembly

The self-assembly of a single monomer can proceed through different packing modes, where one critical assembly state opens access to higher-level elongation stages. This hierarchical mechanism of self-assembly relies on changes in the

non-covalent interactions of monomers as they propagate, either amongst themselves or with their medium.⁷⁸ For example, peptide amphiphiles can self-assemble hierarchically (*i.e.* micelles < nanofibres < fibre bundles) with increasing monomer concentration.⁹⁵ In this case, spherical hydrophobic packing dominates at low concentration, then crowded micelles undergo directional elongation by peptide H-bonding into nanofibres, eventually bundling together through their long multivalent surfaces. Peptoids have also been exploited for the hierarchical assembly of nanostructures, sequentially transitioning from particles to sheets and nanotubes by a "rolling-up and closure" mechanism (Fig. 7A).⁹⁶ Alternatively, glycosylated peptides have shown hierarchical assembly pathways, forming individual supramolecular nanofibres under dilute conditions, while bundling together at high concentration due to water exclusion in crowded environments (Fig. 7B).⁹⁷

We have developed a new class of hierarchically self-assembling peptides, where monomers can amplify certain topologies during an initial one-dimensional (1D) polymerisation stage, subsequently activating a two-dimensional (2D) assembly mode based on hydrophobic enhancement.^{98,99} Here, cyclic peptides with alternating D/L chirality stack by β -sheet-like H-bonding to produce nanotubes, where the polar and hydrophobic domains of the peptide segregate, creating large hydrophobic nanotube surfaces that further assemble as 2D nanosheets in water (Fig. 8A). Computational simulations demonstrated the stronger solvophobic 2D assembly of 1D nanotubes as they grew longer, consistent with an increase in effective hydrophobic surface as monomers cooperatively array non-polar domains (Fig. 8B).¹⁰⁰ Importantly, the positioning of hydrophobic domains around the nanotube determined 2D packing geometry, producing nanotube bilayers or monolayers depending on the angle formed by hydrophobic side chains around the peptide macrocycle.



Fig. 6 Packing gaps in supramolecular peptide assemblies. (A) α -helical monomers with bipyridine pendants on either terminus for segregated peptide and aromatic assembly. Reprinted with permission from ref. 90, copyright 2022, American Chemical Society. (B) Porous assemblies obtained from two β -sheet-forming peptides (green and blue), consisting of double-walled nanotubes. Adapted with permission from ref. 92, copyright 2017, American Chemical Society.

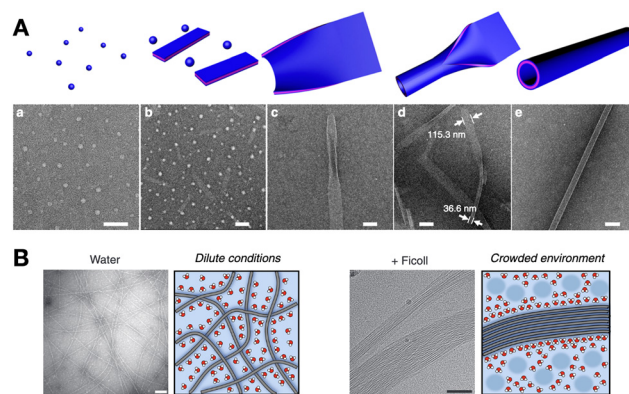


Fig. 7 Hierarchical self-assembly examples. (A) Peptoids capable of assembling spherical, flat 2D and hollow nanotube structures progressively (a–e). Scale bars = 200 nm (a, b and d) and 100 nm (c and e). Reprinted with permission from ref. 96, copyright 2018, Springer Nature. (B) Hierarchical bundling of supramolecular fibres in crowded environments, like in the presence of branched polysaccharides (e.g. FicolI). Scale bars = 100 nm. Adapted with permission from ref. 97, copyright 2019, Springer Nature.



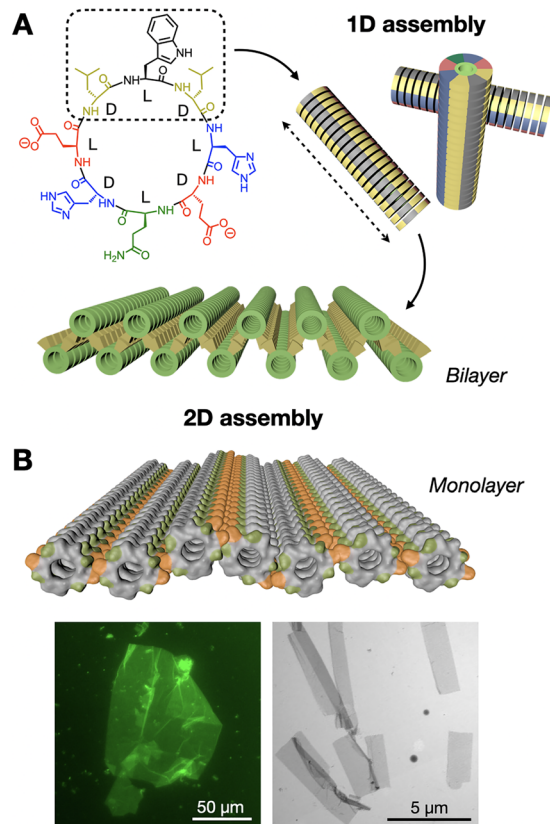


Fig. 8 Hierarchical 1D-to-2D self-assembly of cyclic peptides by hydrophobic amplification. (A) The hydrophobic domain of the peptide monomer (dashed square) is amplified along the one-dimensional (1D) nanotubular axis (dashed arrow), triggering the two-dimensional (2D) assembly of bilayered nanosheets. Adapted with permission from ref. 98, copyright 2020, American Chemical Society. (B) Analogous design, now producing nanotubular monolayers by presenting two hydrophobic domains (in orange) positioned on opposite sides of the nanotubes. Epifluorescence (left) and electron (right) micrographs of monolayered 2D nanosheets. Adapted with permission from ref. 100, copyright 2023, Royal Society of Chemistry.

4. Life-like function

Understanding the molecular and supramolecular principles of biology remains a central focus of interest in contemporary science towards creating synthetic life.¹⁰¹ The bottom-up construction of minimal artificial “cells” (*i.e.* protocells) employs supramolecular building blocks to mimic cellular architectures and functions.^{102–104} In this context, peptides stand out as versatile monomers able to self-assemble as fibres,¹⁰⁵ coacervates¹⁰⁶ and vesicles,¹⁰⁷ to enable the construction of biomimetic systems. Thus, the reproduction of life-like functions by peptide assemblies (*e.g.* confinement in membranes, adaptive fibrillar scaffolds, catalysis, *etc.*) has attracted much attention from the synthetic biology, systems chemistry and prebiotic chemistry communities.¹⁰⁸ All these life-like functions rely on the collective cooperation of peptide monomers, either as static assemblies with biomimetic behaviour, or dynamically changing supramolecular association to adapt to their environment.

4.1. Vesicle and coacervate compartments

The confinement provided by cellular membranes is a defining feature of life, regulating molecular exchange and sustaining essential gradients.¹⁰⁹ Reproducing such compartmentalisation is a central goal in bottom-up protocell development, enabling the production of minimal cell models to investigate transport, energy transduction and adaptive behaviours.¹¹⁰ Schiller *et al.* reported a peptide polymer design, (VPGKG)₄₀-(VPGIG)₃₀, capable of assembling vesicles (Fig. 9A).¹¹¹ In this case, the amphiphilic design of the monomers directs their spatial organisation into bilayered vesicles, where the polarity-based segregation of side chains favours membrane curvature and closure. Das *et al.* recently demonstrated that amphiphilic dipeptides can form dynamic vesicles able to display biomimetic growth, like remodelling and division, outside thermodynamic equilibrium.¹¹² Other examples include giant elastin-like peptide polymer vesicles able to encapsulate biochemical reactions that change vesicle morphology,¹¹³ and short peptide vesicles where inter-monomer affinity determines membrane interaction with the environment.¹¹⁴ Altogether, these systems demonstrate that the cooperative interaction between the assembled units enables emergent behaviours, such as growth, division, and adaptive reshaping, that transcend the properties of individual monomers. However, compared to lipid vesicles, peptide-based membranes continue to confront obstacles in achieving long-term stability and selective permeability,¹¹⁵ posing exciting challenges for further sophistication of cooperative assembly principles and (supra)molecular designs.



Fig. 9 Formation of compartments by self-assembling peptide monomers. (A) Vesicles formed with fluorescently labelled (VPGKG)₄₀-(VPGIG)₃₀ peptide polymer, showing dynamic membrane fusion (red arrow). Scale bars = 5 μm. Reprinted with permission from ref. 111, copyright 2019, American Chemical Society. (B) Co-assembly of tripeptides containing phenylalanine (F) and methionine (M) residues into coacervate droplets. Scale bar = 20 μm. Adapted with permission from ref. 117, copyright 2025, Springer Nature.



While vesicles establish a membrane barrier between their internal and the external medium, membrane-less coacervates allow free molecular exchange with their environment. Thus, coacervates consist of simple compartments produced by disordered peptide aggregation (*i.e.* liquid–liquid phase separation), able to perform life-like functions as protocells with highly dynamic composition and fluidity.¹¹⁶ Caire da Silva *et al.* obtained coacervates by co-assembly of short peptide monomers, which instead produced fibres and solid aggregates in pure samples (Fig. 9B).¹¹⁷ The key concept here is the mixing of very similar tripeptides with a single amino acid relocation, Phe₂Met and MetPhe₂, leading to attractive interactions while distorting crystallinity by sequence mismatch, thus promoting fluid coacervate aggregation. Indeed, it has been established that methionine (Met) can function as a flexible spacer next to fibre-forming hydrophobic cores (*e.g.* Phe), modulating the structural order and fluidity of the resulting assemblies.¹¹⁸

Regarding fuelled out-of-equilibrium designs, Boekhoven *et al.* developed dissipative coacervate droplets formed by RNA–peptide condensation, able to display structural changes such as vacuole formation and fusion.¹¹⁹ The group later designed an analogous complex coacervate system, whose sequential formation and decay could produce daughter droplets, which could grow and divide again by consecutive fueling cycles.¹²⁰ Interestingly, recent evidence that fuelled coacervates do not undergo Ostwald ripening suggests their behaviour can be studied individually, providing a versatile platform to investigate protocellular behaviour and evolution with single droplet resolution and not only in the bulk.¹²¹ Overall, coacervates consist of crowded compartments without a boundary (*i.e.* membrane) that allow non-specific chemical partitioning and changes in the solvation of internalised molecules, where monomers cooperatively drive covalent and supramolecular processes like catalysis^{44,45} and in-coacervate self-assembly.¹²²

4.2. Fibrillar scaffolds

Supramolecular peptide fibres have demonstrated great potential in the structural and functional mimicking of cell and tissue behaviour. These assemblies have been studied as synthetic analogues of the extracellular matrix (ECM) and the cytoskeleton, producing fibrous networks that promote natural cell adhesion and differentiation, as well as structural organisation and function in protocells.^{105,123} Stupp *et al.* have extensively investigated peptide amphiphile nanofibres as ECM-like scaffolds, showing that multivalent cell–fibre interactions are critical for biological activity, and ultimately rely on the cooperative presentation of multiple bioactive monomers on the surface of these supramolecular fibres.¹²⁴ Interestingly, the group found that more dynamic and fluid assemblies are beneficial for bioactivity, probably owing to their higher adaptability to rearrange cell–signalling domains on their surface.¹²⁵ Monomer diffusion within the assembly, and hence biological function, could be adjusted by monomer design to pack either in parallel or antiparallel β -sheet configuration.¹²⁶ Similarly, cooperative multivalent interactions on the surface of these

assemblies can reversibly control hierarchical inter-fibre organisation as bundles, with direct effects on cell behaviour when used as ECM mimics.¹²⁷ While other groups and peptide designs have successfully achieved ECM-like function and derived applications,¹²⁸ the contribution of the Stupp group to the understanding of supramolecular fibres in terms of monomer cooperativity and dynamics sets a solid foundation to guide future progress in biomaterial–cell interfaces.

The ability of peptide assemblies to mimic ECMs can be applied to emulate intracellular fibre networks, like the cytoskeleton, which is responsible for cell structure, motion and organisation.¹²⁹ Despite interesting advances in artificial cytoskeletons for protocell development, like DNA filaments¹³⁰ and diacetylene polymers,¹³¹ peptide designs remain scarce. One of the few examples was reported by Freeman *et al.*, who developed a hybrid peptide–DNA cytoskeleton mimic encapsulated in water-in-oil droplets; a monomer able to mimic the structure and cross-linking of natural actin microfilaments (Fig. 10).¹³² In this work, short diphenylalanine monomers assembled fibres with pendant DNA strands to interconnect peptide filaments into a dynamic network. The resulting cytoskeleton mimic could adapt its structural organisation and induce morphological changes in the droplets, reproducing essential cellular functions by the cooperative restructuring of supramolecular fibre networks.

We have developed a peptide amphiphile monomer capable of fibrillar self-assembly,¹³³ which can be confined in water-in-oil droplets to mimic cytoskeletal structure and function.¹³⁴ In this work, *in situ* production of self-assembling amphiphiles



Fig. 10 Fibre self-assembly inside water-in-oil emulsion droplets. Dipeptide Fmoc-FF-OH (FF) covalently linked to DNA sequences allowed fibre assembly by FF oligomerisation and controlled fibre cross-linking through complementary DNA hybridisation ($A' = 8$ base pair DNA; $A_m - A'_m = 25$ base pair DNA). The presence and length of the DNA linker affect fibre length and spatial organisation. Scale bars = 20 μm . Reprinted with permission from ref. 132, copyright 2024, Springer Nature.





Fig. 11 Confined synthesis and self-assembly of peptide amphiphiles to mimic cytoskeleton structure and function. (A) Fibres are first assembled throughout the droplet interior (0–210 s) to then accumulate at the interface over time (600 s), thus creating a fibrillar cortex. (B) Two-step enzymatic cascade across droplet populations mediated by content exchange *via* connected fibre cortices. Successful reactivity results in the production of a red reporter (300 s). GOx = glucose oxidase, HRP = horseradish peroxidase. Scale bars = 70 μm . Adapted with permission from ref. 134, copyright 2021, Springer Nature.

within droplets could generate fibre networks that over time accumulate at the cortex of these compartments like a cytoskeletal shell (Fig. 11A). Because these monomers are highly anionic, fibrillation can promote the selective uptake of small molecules from the medium based on charge. Neutralisation of these anionic cytoskeletons induced droplet fusion, as fibre cortices stabilise inter-droplet contacts by charge repulsion. However, interfacing cytoskeletons could connect droplets without coalescence, thus maintaining droplet integrity while allowing content exchange, which could be exploited to trigger a two-step enzymatic cascade across droplet populations (Fig. 11B).

5. Summary of peptide designs

In this final section, we classify the examples discussed above based on their supramolecular morphology: either elongated nanofibres and nanotubes, lamellar nanosheets and porous multilayers, or spherical coacervates and vesicles. This summary correlates peptide sequence with supramolecular structure, rationalising nanomaterial fabrication based on monomer design (*e.g.* amino acid composition, peptide derivatisation, *etc.*). A table at the end of this section helps compare all peptide sequences, supramolecular structures, assembly conditions and emergent properties.

5.1. Nanofibres and nanotubes

These assemblies elongate in one dimension of space, usually relying on inter-backbone H-bonding to direct the linear propagation of peptide monomers. As shown in Table 1, most nanofibre and nanotube monomers form linear β -sheets, generally containing hydrophobic residues (*e.g.* Val, Ala, Leu, *etc.*) to promote lateral peptide association by steric zipping as cross- β interfaces (Fig. 1A).¹³⁵ In many designs, charged residues (*e.g.* Glu, Lys, His) generate inter-monomer repulsion on

the surface of the assembly to prevent aggregation,^{34,85,134} while other peptides incorporate both cationic and anionic segments for the electrostatic cross-linking of fibres.^{45,127} The attachment of fatty acids (*e.g.* lauric, palmitic, *etc.*) drives monomer association in water *via* non-directional hydrophobic packing, allowing fatty acid chains to cluster without interfering with the directional (*i.e.* linear) propagation of peptides by H-bonds.^{74,95,125} Interestingly, nanotubes can be obtained from very similar peptide sequences to those producing nanofibres,^{41,45} the former being usually assembled hierarchically from pre-organised structures over time (up to weeks).¹³⁶ Despite all these rational molecular design concepts, fibrillar and tubular peptide assemblies are highly polymorphic, and their final structure strongly depends on kinetic¹³⁷ and energetic parameters (*e.g.* annealing).¹³⁸ As a result, prediction of the supramolecular nanostructure is not possible directly from the monomer sequence alone and also requires systematic screening of environmental conditions and incubation times.

5.2. Nanosheets and porous multilayers

Engineering peptide self-assembly to produce lamellar structures requires fine control over the monomer's geometry to present binding motifs at precise angles. For example, peptides assembling into β -sheets present axial H-bonding contacts perpendicular to side chain binding surfaces (Fig. 1A),⁴⁹ thus allowing the ordered propagation of peptides in these two dimensions. On this basis, enantiomerically pure peptides display consecutive side chains on alternating sides of the β -sheet, unlike peptides made of periodic D–L sequences, which segregate all side chains on one face of the β -sheet, allowing the assembly of porous materials (Fig. 1C)⁹³ and hierarchical nanosheet structures (Fig. 8).^{98,100} Alternatively, helical peptide folds also allow the presentation of side chains at specific angles around the helical axis, as discussed here for the fabrication of porous supramolecular multilayers (Fig. 6A),^{90,91} and applicable to a wide variety of exohelical peptide topologies.¹³⁹ Overall, understanding the geometry of secondary peptide structures is key to rationally designing lamellar assemblies, which serve as scaffolds for positioning the required amino acids at binding and non-binding domains.

5.3. Coacervates and vesicles

The supramolecular architectures discussed in Section 5.1. and 5.2. consist of highly ordered peptide lattices, where monomers self-assemble into defined molecular arrays with restricted conformation and mobility. In contrast, coacervates and vesicles are highly dynamic structures, where monomers can rapidly exchange with the solution and/or diffuse across the assembly. Peptide coacervates are membrane-less droplets formed by aggregation of disordered domains,¹⁴⁰ which can be found in some of the monomers discussed above, like those containing non-peptidic aromatic substituents,^{46,54} flexible linkers,⁵⁵ truncated sequences,¹¹⁷ or unfolded oligopeptides.⁷² Charged peptides can also undergo complex coacervation by disordered aggregation with oppositely charged macromolecules.^{119,122} As their behaviour and stability are



Table 1 Summary of peptide sequences with emergent properties discussed in the previous sections. Unless indicated otherwise (e.g. ^DF), these are all L-amino acids. Abbreviations: n/s (not specified), Nap (naphthalene), Im (imidazole), Catec (catechol), Ar₁ (1-(4-formylbenzyl)-4-phenylpyridin-1-ium), ^βA (beta-alanine), ^{Me}A (2-aminoisobutyric acid), Fmoc (9-fluorenylmethoxycarbonyl), Ac (acetyl), TBDMSO (*tert*-butyldimethylsilyloxy), Bpy (2,2'-bipyridine), Orn (ornithine), Nva (norvaline), GlcNAc (*N*-acetylglucosamine), PEG₂ (diethyleneglycol), DNA (nucleic acid conjugate)

Peptide sequence	Nanostructure	Secondary fold	Emergent property	Assembly trigger	Assembly conc. (mM)	Ref.	
Lauryl-VVAGX-NH ₂ (X = E, K, HH)	Nanofibres	β-sheet	Catalysis	Concentration	0.05	34	
Palmitoyl-H-OH		n/s	Catalysis	Concentration	30	40	
H-KLVFFAE-OH		β-sheet	Catalysis	Coacervation	0.01	45	
Dodecyl = NO-acetyl-F ₃ E ₂ -OH		β-sheet	Catalysis	Concentration	1	74	
Fmoc-FF-OH		β-sheet	Structural amplification	pH	1	6	
H-P(γ-TBDMSO) ^D E(dodecyl)-dodecyl		n/s	Structural amplification	Temperature	10	83	
Ac-F ₃ K-NH ₂		β-sheet	Structural amplification	pH	8	85	
Palmitoyl-A ₄ K ₄ GRADA-NH ₂		β-sheet	Structural amplification	pH	0.75	95	
GlcNAc-(SG) ₂ Q ₂ K(FQ) ₂ FEQ ₂ -NH ₂		β-sheet	Structural amplification	Concentration	5	97	
Ac-A ₆ YD-OH		n/s	Life-like	Concentration	3	114	
Palmitoyl-V ₂ A ₂ E ₄ IKVAV-NH ₂	β-sheet	Life-like	Concentration	6	125		
Palmitoyl-V ₃ A ₃ E ₃ -NH ₂ , H-E ₃ A ₃ -V ₃ K(lauryl)-NH ₂	β-sheet	Life-like	Concentration	10	126		
Palmitoyl-V ₃ A ₃ E ₃ K ₃ -PEG ₂ -DNA, palmitoyl-V ₃ A ₃ E ₃ K ₃ -NH ₂	β-sheet	Life-like	DNA hybridisation	0.5	127		
Fmoc-FF-OH, Fmoc-FF-PEG ₂ -DNA	Nanotubes	β-sheet	Life-like	DNA hybridisation	2	132	
Alkyl = NO-acetyl-V ₂ A ₂ E ₂ -NH ₂		β-sheet	Life-like	Concentration	10	133	
Octyl = NO-capryloyl-V ₂ A ₂ E ₂ -NH ₂		β-sheet	Life-like	Concentration	1	134	
Im-KLVFFAL-NH ₂		β-sheet	Catalysis	Concentration	1	41	
Nap-FFXH-OH (X = D, H, S, R, K)		β-sheet	Catalysis	pH	1.6–33	47	
Ac-I ₄ ^D KK-NH ₂		β-sheet	Structural amplification	Concentration	16	80	
H _n FF (n = 1–20)		β-sheet	Catalysis	pH	n/s	49	
cyclo(W ^D LH ^D DEQ ^D HE ^D L)		β-sheet	Structural amplification	Concentration	0.1	98	
cyclo(W ^D LE ^D HL ^D WL ^D EH ^D L)		β-sheet	Structural amplification	Concentration	0.1	100	
Bpy-L ^{Me} AA ^{Me} AL ^{Me} AQ ^{Me} AL-Bpy		α-helix	Structural amplification	Temperature	12	90	
Fmoc-P ₄ -NH ₂	Porous multilayer	Helix	Structural amplification	Temperature	40	91	
cyclo[(KLVFFAEOrn) ₂]		β-sheet	Structural amplification	Crystallisation	5	92	
H-F ^D NvaF-OH		β-sheet	Structural amplification	Concentration	8	93	
H- ^D F(4-fluoro)F-OH		β-sheet	Structural amplification	Concentration	38	94	
H-KVYFSIPWRVPM-NH ₂		β-sheet	Catalysis	Ionic strength	0.66	44	
Catec-SDLVFFH-NH ₂		β-sheet	Catalysis	Concentration	0.6	46	
Ar ₁ - ^β AFF ^{Me} A-NH ₂		n/s	Catalysis	Concentration	20	54	
(H-FF) ₂ -cystamine		n/s	Catalysis	pH, concentration	1.35	55	
Oligo(C)		n/s	Catalysis	Concentration	1	72	
H-FFM-OMe, H-MFF-OMe		n/s	Life-like	pH, concentration	2.4	117	
Ac-FRGRGRGD-OH	Coacervates	n/s	Life-like	Electrostatic complexation	23	119	
H-LVFFAR ₉ -OH		β-sheet	Life-like	Electrostatic complexation	5	122	
(VPGKG) ₄₀ (VPGIG) ₃₀		Vesicles	n/s	Life-like	Concentration	0.001–0.05	111
[(VPGRG) ₅ (VPGQG) ₅] ₂ (VPGFG) ₂₀			Random coil	Life-like	Concentration	0.3	113

determined by weak supramolecular interactions, coacervates can adapt their properties to environmental conditions that affect these bonds (e.g. temperature, pH, etc.). In this regard, peptide coacervates have attracted much attention as dynamic protocell models and life-like materials,^{102,140} which can accumulate and freely exchange substances with the surroundings without the permeability restrictions of a lipid membrane. Alternatively, peptide vesicles can be assembled from large amphiphilic peptide polymers,^{111,113} which create an impermeable boundary to control concentration gradients and molecular composition across their membrane.

6. Conclusions and outlook

This review puts in perspective the supramolecular cooperativity of peptide nanostructures, whereby assembled peptide

monomers show emergent properties that transcend the sum of their individual features. We have shown functional responses emerging from collective monomer behaviour, such as catalysis, structural amplification, hierarchical assembly pathways and life-like function, amongst others. These phenomena are usually reviewed and discussed individually, as isolated topics with little connection between the fields and applications covered herein. We believe that integrating advances in monomer design, applications and mechanistic understanding into a single broader topic, here termed *emergent properties*, would benefit all these areas of research.

Our contributions to these areas have been highlighted at the end of each section, including autocatalytic systems, hierarchical self-assembling monomers and functional cytoskeleton mimics. We have studied a variety of peptide designs and supramolecular architectures that have contributed to advancing peptide nanotechnology, both conceptually and in



- 41 B. Sarkhel, A. Chatterjee and D. Das, *J. Am. Chem. Soc.*, 2020, **142**, 4098–4103.
- 42 A. Chatterjee, C. Mahato and D. Das, *Angew. Chem., Int. Ed.*, 2021, **60**, 202–207.
- 43 T. O. Omosun, M.-C. Hsieh, W. S. Childers, D. Das, A. K. Mehta, N. R. Anthony, T. Pan, M. A. Grover, K. M. Berland and D. G. Lynn, *Nat. Chem.*, 2017, **9**, 805–809.
- 44 D. Q. P. Reis, S. Pereira, A. P. Ramos, P. M. Pereira, L. Morgado, J. Calvário, A. O. Henriques, M. Serrano and A. S. Pina, *Nat. Commun.*, 2024, **15**, 9368.
- 45 W. Li, Y. Zhou, T. Tong, S. He, C. Wang, X. Zhang, X.-Y. Cao, L. Yang and Z.-Q. Tian, *ACS Nano*, 2025, **19**, 2306–2314.
- 46 A. Singh, J. Chakraborty, S. Pal and D. Das, *Proc. Natl. Acad. Sci. U. S. A.*, 2024, **121**, e2321396121.
- 47 Y. Zhang, X. Tian and X. Li, *J. Mater. Chem. B*, 2022, **10**, 3716–3722.
- 48 Z. Lengyel, C. M. Rufo, Y. S. Moroz, O. V. Makhlynets and I. V. Korendovych, *ACS Catal.*, 2018, **8**, 59–62.
- 49 Q. Liu, K. Wan, Y. Shang, Z.-G. Wang, Y. Zhang, L. Dai, C. Wang, H. Wang, X. Shi, D. Liu and B. Ding, *Nat. Mater.*, 2021, **20**, 395–402.
- 50 M. Diaz-Caballero, S. Navarro, M. Nuez-Martinez, F. Peccati, L. Rodriguez-Santiago, M. Sodupe, F. Teixidor and S. Ventura, *ACS Catal.*, 2021, **11**, 595–607.
- 51 N. Singh, M. Tena-Solsona, J. F. Miravet and B. Escuder, *Isr. J. Chem.*, 2015, **55**, 711–723.
- 52 M. Tena-Solsona, J. Nanda, S. Diaz-Oltra, A. Chotera, G. Ashkenasy and B. Escuder, *Chem. – Eur. J.*, 2016, **22**, 6687–6694.
- 53 N. Singh and B. Escuder, *Chem. – Eur. J.*, 2017, **23**, 9946–9951.
- 54 S. Bal, S. Gupta, C. Mahato and D. Das, *Angew. Chem., Int. Ed.*, 2025, **64**, e202505296.
- 55 M. Abbas, W. P. Lipiński, K. K. Nakashima, W. T. S. Huck and E. Spruijt, *Nat. Chem.*, 2021, **13**, 1046–1054.
- 56 A. I. Hanopolskyi, V. A. Smaliak, A. I. Novichkov and S. N. Semenov, *ChemSystemsChem*, 2021, **3**, e2000026.
- 57 H. P. Lesutis, R. Gläser, C. L. Liotta and C. A. Eckert, *Chem. Commun.*, 1999, 2063–2064.
- 58 M. G. Howlett and S. P. Fletcher, *Nat. Rev. Chem.*, 2023, **7**, 673–691.
- 59 D. H. Lee, J. R. Granja, J. A. Martinez, K. Severin and M. R. Ghadiri, *Nature*, 1996, **382**, 525–528.
- 60 Z. Dadon, N. Wagner, S. Alasibi, M. Samiappan, R. Mukherjee and G. Ashkenasy, *Chem. – Eur. J.*, 2015, **21**, 648–654.
- 61 S. K. Rout, D. Rhyner, R. Riek and J. Greenwald, *Chem. – Eur. J.*, 2022, **28**, e202103841.
- 62 A. K. Bandela, N. Wagner, H. Sadihov, S. Morales-Reina, A. Chotera-Ouda, K. Basu, R. Cohen-Luria, A. de la Escosura and G. Ashkenasy, *Proc. Natl. Acad. Sci. U. S. A.*, 2021, **118**, e2015285118.
- 63 C. Chen, J. Tan, M.-C. Hsieh, T. Pan, J. T. Goodwin, A. K. Mehta, M. A. Grover and D. G. Lynn, *Nat. Chem.*, 2017, **9**, 799–804.
- 64 S. Otto, *Acc. Chem. Res.*, 2022, **55**, 145–155.
- 65 J. M. A. Carnall, C. A. Waudby, A. M. Belenguer, M. C. A. Stuart, J. J.-P. Peyralans and S. Otto, *Science*, 2010, **327**, 1502–1506.
- 66 M. J. Eleveld, Y. Geiger, J. Wu, A. Kiani, G. Schaeffer and S. Otto, *Nat. Chem.*, 2025, **17**, 132–140.
- 67 M. Altay, Y. Altay and S. Otto, *Angew. Chem., Int. Ed.*, 2018, **57**, 10564–10568.
- 68 P. Adamski, M. Eleveld, A. Sood, Á. Kun, A. Szilágyi, T. Czárán, E. Szathmáry and S. Otto, *Nat. Rev. Chem.*, 2020, **4**, 386–403.
- 69 A. Kahana and D. Lancet, *Nat. Rev. Chem.*, 2021, **5**, 870–878.
- 70 Z. Zhang, M. G. Howlett, E. Silvester, P. Kukura and S. P. Fletcher, *J. Am. Chem. Soc.*, 2024, **146**, 18262–18269.
- 71 I. Colomer, S. M. Morrow and S. P. Fletcher, *Nat. Commun.*, 2018, **9**, 2239.
- 72 M. Matsuo and K. Kurihara, *Nat. Commun.*, 2021, **12**, 5487.
- 73 S. Patra, B. Sharma and S. J. George, *J. Am. Chem. Soc.*, 2025, **147**, 16027–16037.
- 74 I. Turcan and I. Insua, *ChemSystemsChem*, 2025, **7**, e202400094.
- 75 L. Calahorra-Rio and I. Colomer, *ChemSystemsChem*, 2025, **7**, e00025.
- 76 Z. Chen, Z. Chi, Y. Sun and Z. Lv, *Chirality*, 2021, **33**, 618–642.
- 77 T. Vijayakanth, S. Dasgupta, P. Ganatra, S. Rencus-Lazar, A. V. Desai, S. Nandi, R. Jain, S. Bera, A. I. Nguyen, E. Gazit and R. Misra, *Chem. Soc. Rev.*, 2024, **53**, 3640–3655.
- 78 B. B. Gerbelli, S. V. Vassiliades, J. E. U. Rojas, J. N. B. D. Pelin, R. S. N. Mancini, W. S. G. Pereira, A. M. Aguilar, M. Venanzi, F. Cavalieri, F. Giuntini and W. A. Alves, *Macromol. Chem. Phys.*, 2019, **220**, 1900085.
- 79 Y. Zheng, L. Yu, Y. Zou, Y. Yang and C. Wang, *Nano Lett.*, 2019, **19**, 5403–5409.
- 80 H. Xu, K. Qi, C. Zong, J. Deng, P. Zhou, X. Hu, X. Ma, D. Wang, M. Wang, J. Zhang, S. M. King, S. E. Rogers, J. R. Lu, J. Yang and J. Wang, *Small*, 2024, **20**, e2304424.
- 81 C. Zheng, S. Lin, C. Hu, Y. Li, B. Li and Y. Yang, *N. J. Chem.*, 2020, **44**, 20726–20733.
- 82 M. Qin, Y. Zhang, C. Xing, L. Yang, C. Zhao, X. Dou and C. Feng, *Chem. – Eur. J.*, 2021, **27**, 3119–3129.
- 83 S. Bhowmick, L. Zhang, G. Ouyang and M. Liu, *ACS Omega*, 2018, **3**, 8329–8336.
- 84 C. Gao, Z. Zhu, S. Li, Z. Xi, Q. Sun, J. Han and R. Guo, *Chin. Chem. Lett.*, 2025, **36**, 109968.
- 85 K. Qi, H. Qi, M. Wang, X. Ma, Y. Wang, Q. Yao, W. Liu, Y. Zhao, J. Wang, Y. Wang, W. Qi, J. Zhang, J. R. Lu and H. Xu, *Nat. Commun.*, 2024, **15**, 6186.
- 86 G. Liu, X. Li, J. Sheng, P.-Z. Li, W. K. Ong, S. Z. F. Phua, H. Ågren, L. Zhu and Y. Zhao, *ACS Nano*, 2017, **11**, 11880–11889.
- 87 N. Picois, L. Boderio, P. Milbeo, T. Brigaud and G. Chaume, *Chem. – Eur. J.*, 2024, **30**, e202400540.
- 88 A. R. A. Palmans and E. W. Meijer, *Angew. Chem., Int. Ed.*, 2007, **46**, 8948–8968.
- 89 A. Desmarchelier, M. Raynal, P. Brocorens, N. Vanthuyne and L. Bouteiller, *Chem. Commun.*, 2015, **51**, 7397–7400.
- 90 S. L. Heinz-Kunert, A. Pandya, V. T. Dang, P. N. Tran, S. Ghosh, D. McElheny, B. D. Santarsiero, Z. Ren and A. I. Nguyen, *J. Am. Chem. Soc.*, 2022, **144**, 7001–7009.
- 91 D. F. Brightwell, G. Truccolo, K. Samanta, E. J. Fenn, S. J. Holder, H. J. Shepherd, C. S. Hawes and A. Palma, *Chem. – Eur. J.*, 2022, **28**, e202202368.
- 92 K. H. Chen, K. A. Corro, S. P. Le and J. S. Nowick, *J. Am. Chem. Soc.*, 2017, **139**, 8102–8105.
- 93 A. M. Garcia, D. Iglesias, E. Parisi, K. E. Styan, L. J. Waddington, C. Deganutti, R. D. Zorzi, M. Grassi, M. Melchionna, A. V. Vargiu and S. Marchesan, *Chem*, 2018, **4**, 1862–1876.
- 94 S. Kralj, O. Bellotto, E. Parisi, A. M. Garcia, D. Iglesias, S. Semeraro, C. Deganutti, P. D'Andrea, A. V. Vargiu, S. Geremia, R. D. Zorzi and S. Marchesan, *ACS Nano*, 2020, **14**, 16951–16961.
- 95 Y. Chen, H. X. Gan and Y. W. Tong, *Macromolecules*, 2015, **48**, 2647–2653.
- 96 H. Jin, Y.-H. Ding, M. Wang, Y. Song, Z. Liao, C. J. Newcomb, X. Wu, X.-Q. Tang, Z. Li, Y. Lin, F. Yan, T. Jian, P. Mu and C.-L. Chen, *Nat. Commun.*, 2018, **9**, 270.
- 97 A. Restuccia, D. T. Seroski, K. L. Kelley, C. S. O'Bryan, J. J. Kurian, K. R. Knox, S. A. Farhadi, T. E. Angelini and G. A. Hudalla, *Commun. Chem.*, 2019, **2**, 53.
- 98 I. Insua and J. Montenegro, *J. Am. Chem. Soc.*, 2020, **142**, 300–307.
- 99 S. Diaz, I. Insua, G. Bhak and J. Montenegro, *Chem. – Eur. J.*, 2020, **26**, 14765–14770.
- 100 I. Insua, A. Cardellini, S. Diaz, J. Bergueiro, R. Capelli, G. M. Pavan and J. Montenegro, *Chem. Sci.*, 2023, **14**, 14074–14081.
- 101 C. M. E. Kriebisch, O. Bantysch, L. B. Pellejero, A. Belluati, E. Bertolin, K. Dai, M. de Roy, H. Fu, N. Galvanetto, J. M. Gibbs, S. S. Gomez, G. Granatelli, A. Griffo, M. Guix, C. O. Gurdap, J. Harth-Kitzerow, I. S. Haugerud, G. Häfner, P. Jaiswal, S. Javed, A. Karimi, S. Kato, B. A. K. Kriebisch, S. Laha, P.-W. Lee, W. P. Lipinski, T. Matreux, T. C. T. Michaels, E. Poppleton, A. Ruf, A. D. Sloodbeek, I. B. A. Smokers, H. Soria-Carrera, A. Sorrenti, M. Stasi, A. Stevenson, A. Thatte, M. Tran, M. H. I. van Haren, H. D. Vuijk, S. F. J. Wickham, P. Zambrano, K. P. Adamala, K. Alim, E. S. Andersen, C. Bonfio, D. Braun, E. Frey, U. Gerland, W. T. S. Huck, F. Jülischer, N. Laohakunakorn, L. Mahadavan, S. Otto, J. Saenz, P. Schwillke, K. Göpflich, C. A. Weber and J. Boekhoven, *Chem*, 2025, **11**, 102399.
- 102 I. Insua and J. Montenegro, *Chem*, 2020, **6**, 1652–1682.
- 103 P. Schwillke, J. Spatz, K. Landfester, E. Bodenschatz, S. Herminghaus, V. Sourjik, T. J. Erb, P. Bastiaens, R. Lipowsky, A. Hyman, P. Dabrock, J. Baret, T. Vidakovic-Koch, P. Bieling, R. Dimova, H. Mutschler, T. Robinson, T.-Y. D. Tang, S. Wegner and C. Sundmacher, *Angew. Chem., Int. Ed.*, 2018, **57**, 13382–13392.
- 104 B. C. Buddingh and J. C. M. van Hest, *Acc. Chem. Res.*, 2017, **50**, 769–777.
- 105 A. Sanchez-Fernandez, I. Insua and J. Montenegro, *Commun. Chem.*, 2024, **7**, 223.



- 106 M. Abbas, W. P. Lipiński, J. Wang and E. Spruijt, *Chem. Soc. Rev.*, 2021, **50**, 3690–3705.
- 107 V. Haridas, *Acc. Chem. Res.*, 2021, **54**, 1934–1949.
- 108 M. Frenkel-Pinter, M. Samanta, G. Ashkenasy and L. J. Leman, *Chem. Rev.*, 2020, **120**, 4707–4765.
- 109 J. C. Blain and J. W. Szostak, *Biochemistry*, 2014, **83**, 615–640.
- 110 E. Floris, A. Piras, L. Dall'Asta, A. Gamba, E. Hirsch and C. C. Campa, *Comput. Struct. Biotechnol. J.*, 2021, **19**, 3225–3233.
- 111 A. Schreiber, M. C. Huber and S. M. Schiller, *Langmuir*, 2019, **35**, 9593–9610.
- 112 S. Jha, S. Roy, A. Reja, A. K. Singh, L. Roy and D. Das, *Chem*, 2025, 102630.
- 113 T. Frank, K. Vogele, A. Dupin, F. C. Simmel and T. Pirzer, *Chem. – Eur. J.*, 2020, **26**, 17356–17360.
- 114 K. Kornmueller, B. Lehofer, C. Meindl, E. Fröhlich, G. Leitinger, H. Amenitsch and R. Prassl, *Biomacromolecules*, 2016, **17**, 3591–3601.
- 115 K. Tao, A. Levin, L. Adler-Abramovich and E. Gazit, *Chem. Soc. Rev.*, 2016, **45**, 3935–3953.
- 116 C. D. Crowe and C. D. Keating, *Interface Focus*, 2018, **8**, 20180032.
- 117 S. Cao, P. Zhou, G. Shen, T. Ivanov, X. Yan, K. Landfester and L. C. da Silva, *Nat. Commun.*, 2025, **16**, 2407.
- 118 J. C. Heiby, B. Goretzki, C. M. Johnson, U. A. Hellmich and H. Neuweiler, *Nat. Commun.*, 2019, **10**, 4378.
- 119 C. Donau, F. Späth, M. Sosson, B. A. K. Kriebisch, F. Schnitter, M. Tena-Solsona, H.-S. Kang, E. Salibi, M. Sattler, H. Mutschler and J. Boekhoven, *Nat. Commun.*, 2020, **11**, 5167.
- 120 M. Wenisch, Y. Li, M. G. Braun, L. Eylert, F. Späth, S. M. Poprawa, B. Rieger, C. V. Synatschke, H. Niederholtmeyer and J. Boekhoven, *Chem*, 2025, **11**, 102578.
- 121 K. K. Nakashima, M. H. I. van Haren, A. A. M. André, I. Robu and E. Spruijt, *Nat. Commun.*, 2021, **12**, 3819.
- 122 A. Jain, S. Kassem, R. S. Fisher, B. Wang, T.-D. Li, T. Wang, Y. He, S. Elbaum-Garfinkle and R. V. Uljijn, *J. Am. Chem. Soc.*, 2022, **144**, 15002–15007.
- 123 K. S. Hellmund and B. Koks, *Front. Chem.*, 2019, **7**, 172.
- 124 S. S. Lee, T. Fyrner, F. Chen, Z. Á. Alvarez, E. Sleep, D. S. Chun, J. A. Weiner, R. W. Cook, R. D. Freshman, M. S. Schallmo, K. M. Katchko, A. D. Schneider, J. T. Smith, C. Yun, G. Singh, S. Z. Hashmi, M. T. McClendon, Z. Yu, S. R. Stock, W. K. Hsu, E. L. Hsu and S. I. Stupp, *Nat. Nanotechnol.*, 2017, **12**, 821–829.
- 125 Z. Álvarez, A. N. Kolberg-Edelbrock, I. R. Sasselli, J. A. Ortega, R. Qiu, Z. Syrgiannis, P. A. Mirau, F. Chen, S. M. Chin, S. Weigand, E. Kiskinis and S. I. Stupp, *Science*, 2021, **374**, 848–856.
- 126 R. Qiu, W. Ji, Z. Alvarez, H. Sai, Z. Gao, F. Chen, A. A. Linton, N. J. Lanzetta, A. M. Goodwin, H. J. Brecount, J. Li, J. Inglis, S. Kurapaty, S. R. Stock, W. K. Hsu, L. C. Palmer, E. L. Hsu and S. I. Stupp, *J. Am. Chem. Soc.*, 2025, **147**, 21586–21599.
- 127 R. Freeman, M. Han, Z. Álvarez, J. A. Lewis, J. R. Wester, N. Stephanopoulos, M. T. McClendon, C. Lynsky, J. M. Godbe, H. Sangji, E. Luijten and S. I. Stupp, *Science*, 2018, **362**, 808–813.
- 128 C. Ligorio and A. Mata, *Nat. Rev. Bioeng.*, 2023, **1**, 1–19.
- 129 D. A. Fletcher and R. D. Mullins, *Nature*, 2010, **463**, 485–492.
- 130 P. Zhan, K. Jahnke, N. Liu and K. Göpfrich, *Nat. Chem.*, 2022, **14**, 958–963.
- 131 S. Novosedlik, F. Reichel, T. van Veldhuisen, Y. Li, H. Wu, H. Janssen, J. Guck and J. van Hest, *Nat. Chem.*, 2025, **17**, 356–364.
- 132 M. L. Daly, K. Nishi, S. J. Klawa, K. Y. Hinton, Y. Gao and R. Freeman, *Nat. Chem.*, 2024, **16**, 1229–1239.
- 133 R. Booth, I. Insua, G. Bhak and J. Montenegro, *Org. Biomol. Chem.*, 2019, **17**, 1984–1991.
- 134 R. Booth, I. Insua, S. Ahmed, A. Rioboo and J. Montenegro, *Nat. Commun.*, 2021, **12**, 6421.
- 135 A. W. P. Fitzpatrick, *Proc. Natl. Acad. Sci. U. S. A.*, 2013, **110**, 5468–5473.
- 136 X. Ma, Y. Zhao, C. He, X. Zhou, H. Qi, Y. Wang, C. Chen, D. Wang, J. Li, Y. Ke, J. Wang and H. Xu, *Nano Lett.*, 2021, **21**, 10199–10207.
- 137 M. Wilkinson, Y. Xu, D. Thacker, A. I. P. Taylor, D. G. Fisher, R. U. Gallardo, S. E. Radford and N. A. Ranson, *Cell*, 2023, **186**, 5798.
- 138 F. Wang, O. Gnewou, S. Wang, T. Osinski, X. Zuo, E. H. Egelman and V. P. Conticello, *Matter*, 2021, **4**, 3217–3231.
- 139 J. M. Martínez-Parra, R. Gómez-Ojea, G. A. Daudey, M. Calvelo, H. Fernández-Caro, J. Montenegro and J. Bergueiro, *Nat. Commun.*, 2024, **15**, 6987.
- 140 J. Yuan, Y. Yang, K. Dai, R. Fakhruddin, H. Li, P. Zhou, C. Yuan and X. Yan, *ACS Appl. Mater. Interfaces*, 2025, **17**, 27697–27712.

